Microreactors

Deutsche Ausgabe: DOI: 10.1002/ange.201607406
Internationale Ausgabe: DOI: 10.1002/anie.201607406

Nanofibrillar Stimulus-Responsive Cholesteric Microgels with Catalytic Properties

*Sangho Cho[+], Yunfeng Li[+], Minseok Seo, and Eugenia Kumacheva**

Abstract: *We report composite stimulus-responsive cholesteric catalytically active microgels derived from filamentous supramolecular building blocks: cellulose nanocrystals (CNCs). The variation in the microgel dimensions and pitch in response to the change in ambient conditions was governed by the polymer component. The cholesteric morphology of the microgels resulted from the self-organization of CNCs in spherical confinement. The microgels exhibited excellent structural integrity and functioned as microreactors in catalytic hydrolysis reactions and in the synthesis of metal nanoparticles. Because of these collective properties, the reported microgels show much promise for application in the design of functional responsive materials.*

Polymer microgels are submicrometer- to micrometer-sized particles with a network structure swollen in a solvent. Microgels are an important class of soft-matter materials with applications in drug delivery,[1] sensing,[2] photonics,[3] template-based synthesis,[4] cell culture,[5] and separation and purification[6] technologies. Typically, polymer microgels, as well as macroscopic gels, are generated by chemical or physical cross-linking of small molecules to form a network structure.

Biologically diverse hydrogels formed by filamentous supramolecular building blocks have attracted the interest of the materials science community owing to their nonlinear viscoelastic hydrogel behavior, large pore size, good transport properties, and thermal stability.[7] These features have stimulated research efforts to reproduce their structure in nanofibrillar man-made hydrogels formed by wormlike supramolecular species, such as block-copolymer micelles[8] or assemblies of peptide amphiphiles.[9]

Filament-like nanoparticles (NPs) can also form hydrogels,[10] which would alleviate the need for the synthesis of block copolymers or peptide amphiphiles. In particular, rodlike cellulose nanocrystals (CNCs) are attractive building blocks for nanofibrillar hydrogels. The use of CNCs offers two interesting and potentially useful features. First, hydroxy groups of the CNC surface can be used in catalytic reactions[11] and for the reduction of metal ions.[12] Second, CNCs show a unique ability to form a cholesteric (Ch) liquid-crystalline phase (Ch-CNC). This feature has been utilized for the preparation of films of stimuli-responsive photonic hydrogels by the photopolymerization of a mixture of CNCs and a hydrogel monomer precursor.[13] Microgels derived from Ch-CNC phases have not been reported, although they can exhibit spherical-confinement-induced morphologies[14] and can be used as microreactors owing to their small size and large surface area.[15]

Herein, we report nanofibrillar, composite stimulus-responsive CNC-derived microgels with a Ch structure. Microgels with a narrow size distribution were prepared by microfluidic (MF) emulsification of a mixture of the Ch-CNC phase, a monomer, and a cross-linker, followed by the photopolymerization of the monomer in the precursor droplets and subsequent transfer of the resultant microgels into an aqueous medium. The morphology of the microgels was controlled by their size and was altered from the spherical concentric to the bipolar planar Ch structure by reducing the droplet dimensions. The structural stability of the Ch microgels was established by microgel drying and subsequent reswelling in water. The microgels exhibited collective properties of CNCs and polymer hydrogels. The stimulus-responsive nature of the microgels was governed by the polymer component and was evidenced by tuning the microgel size and pitch at varying ionic strength and temperature of the ambient medium. The microgels exhibited catalytic performance in a hydrolysis reaction and were used for the in situ synthesis of plasmonic Ag NPs. The resulting Ag NP-laden microgels exhibited catalytic activity in a reduction reaction.

An aqueous 6.2 wt % suspension of CNCs with an average length and diameter of 183 and 23 nm, respectively, was equilibrated for 28 days to enable its phase separation into an isotropic top phase and a Ch bottom phase, in agreement with earlier reports.[14] The Ch phase was separated and concentrated to 8.2 wt % by the evaporation of water. This suspension was mixed with 2-hydroxyethyl acrylate (HEA), poly(ethylene glycol) dimethacrylate (PEGDMA), and Irgacure 2595, that is, a monomer, a cross-linker, and a photoinitiator, respectively.

By the use of a microfluidic flow-focusing device,[16] the mixed suspension was emulsified in 3-ethoxy-1,1,1,2,3,4,4,5,5,6,6,6-dodecafluoro-2-(trifluoromethyl)hexane (F-oil) containing 1.0 wt % of a surfactant[17] triblock copolymer.

[*] Dr. S. Cho,[+] Dr. Y. Li,[+] Dr. M. Seo, Prof. E. Kumacheva
Department of Chemistry, University of Toronto
80 Saint George Street, Toronto, Ontario M5S 3H6 (Canada)
E-mail: ekumache@chem.utoronto.ca
Prof. E. Kumacheva
Department of Chemical Engineering and Applied Chemistry
University of Toronto
200 College Street, Toronto, Ontario M5S 3E5 (Canada)
Prof. E. Kumacheva
Institute of Biomaterials and Biomedical Engineering
University of Toronto
4 Taddle Creek Road, Toronto, Ontario M5S 3G9 (Canada)
[+] These authors contributed equally.

Supporting information for this article can be found under: http://dx.doi.org/10.1002/anie.201607406.

The diameter, D, of the droplets was controlled between 20 and 130 μm by varying the MF design (see Figure S1 in the Supporting Information) and by changing the flow-rate ratio of the F-oil to the aqueous suspension from 0.1:0.015 to 0.5:0.1. The droplets had polydispersity (defined as the standard deviation in the droplet diameter divided by the mean droplet diameter) below 3.0% (see Figure S2). The droplets were collected and stored in a sealed glass capillary tube.

Figure 1 a,b shows representative cross-polarized optical microscopy (POM) images of precursor droplets with a diameter D of 126 and 20 μm, respectively. The corresponding bright-field (BF) images are shown as insets. The POM images of the droplets with $80 \leq D \leq 230$ μm showed characteristic Ch structural features with a Maltese cross and alternating concentric bright and dark rings. The tangential surface anchoring of the director at the droplet–oil interface led to the spherical packing of CNCs at the droplet–oil interface and propagation of the Ch structure toward the droplet center. These features were consistent with earlier experimental observations for Ch-CNC droplets[14] and numerical simulations[18] of thermotropic Ch droplets. The average pitch, P, of these droplets (measured as the double distance between two adjacent concentric rings) was 5.4 μm. Droplets with $D < 40$ μm showed a stripe pattern characteristic of flattened Ch-CNC layers trapped between two diametrically opposite poles (a bipolar structure). The average pitch, P, of the Ch structure in these droplets (determined as the double distance between two adjacent stripes) was 6.9 μm (Figure 1 b).

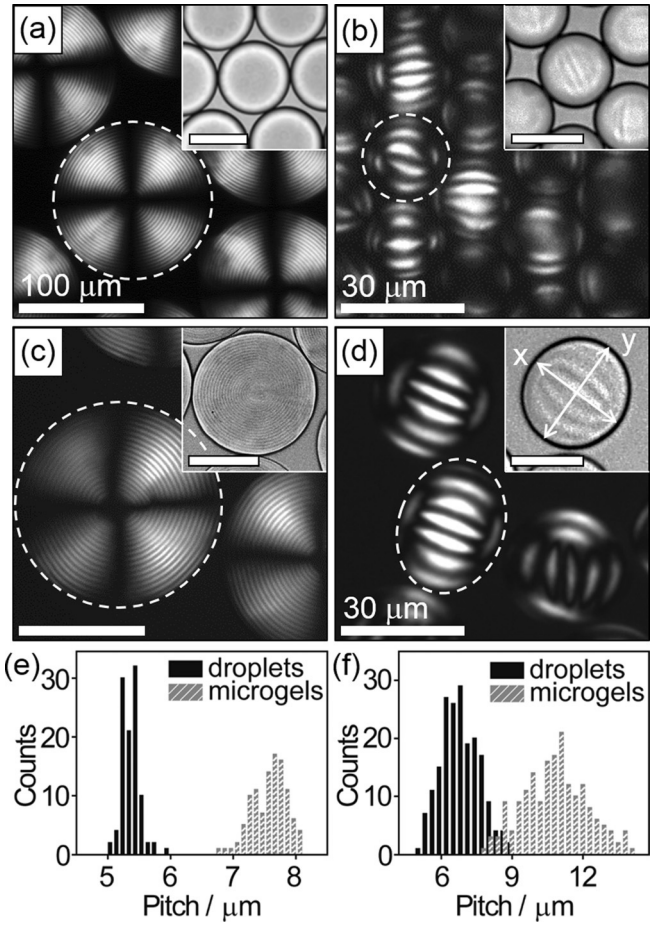

Figure 1. a–d) POM images of Ch-CNC droplets in F-oil (a,b) and microgels in water (c,d). Dashed lines show the contours of droplets (a,b) and microgels (c,d). The insets show corresponding BF images of the precursor droplets (a,b) and microgels (c,d). The inset in (d) shows a prolate spheroid formed by a small microgel. Scale bars are 100 μm in insets (a,c) and 20 μm in insets (b,d). e,f) Distribution of P in large microgels and the corresponding precursor droplets (e) and "small" microgels and the corresponding precursor droplets (f).

The droplets were subjected to UV irradiation (400 W, $\lambda =$ 330–380 nm) for 10–15 min to polymerize HEA and in this manner transform the droplets into Ch-CNC microgels. Herein, we refer to the composite microgels containing cross-linked poly(2-hydroxyethyl acrylate) (PHEA) and CNCs as Ch-CNC microgels. Following polymerization, the Ch structure of the microgels was preserved, with a weak ($< 4\%$) change in the microgel size and pitch (see Figure S3). Herein, we refer to the microgels with a concentric Ch morphology (Figure 1 c) and a stripe pattern (Figure 1 d) as "large" and "small" microgels, respectively. Upon transfer into deionized water, large microgels swelled, and their D and P values increased from 126 to 181 μm and from 5.4 to 7.6 μm, respectively. Expansion of these microgels was isotropic, with their spherical microgel shape and Ch structure well preserved (Figure 1 c,d; see also Figure S2 c). The extent of microgel swelling depended on the ratio of the monomer to the cross-linker concentration, which determined the polymer cross-linking density (see Figure S4).

Interestingly, small microgels with a bipolar structure exhibited anisotropic swelling in water, thus resulting in the generation of microgels with the shape of prolate spheroids. The aspect ratio of such microgels, determined as the ratio of the polar to equatorial lengths along the y and x axis (Figure 1 d; see also Figure S2 d), varied from 1.02 to 1.18 (see Figure S2 g), with P increasing from 6.9 to 10.8 μm (Figure 1 f). Microgel swelling was limited along the direction parallel to the CNC layers,[19] whereas stronger expansion occurred along the direction perpendicular to the CNC layers.

The structural integrity of the Ch-CNC microgels was studied for the large microgels by drying and subsequent reswelling in water. In the case of anisotropic drying, the Ch-CNC microgels deposited on a glass slide were dried under ambient conditions (Figure 2; see also Figure S5). The microgels shrank and flattened, largely losing their three-dimensional concentric Ch structure; however, upon equilibration in water for 24 h, they restored their original dimensions, their spherical shape, and the Ch morphology, with $P < 10\%$ larger than in the original microgels (Figure 2 c,d; see also Figure S5 c). An isotropic drying method was also used, whereby dispersions of Ch-CNC microgels were freeze-dried in liquid nitrogen. After equilibration in water for 24 h, the dried microgels restored their dimensions, shape, and morphology, and exhibited no significant change in D and P in comparison with the pristine microgels (see Figure S6).

We examined the stimuli-responsive nature of the large Ch-CNC microgels by changing the ionic strength of the ambient aqueous phase. Upon the addition of NaCl at concentrations up to 6 M, the microgels shrank and their

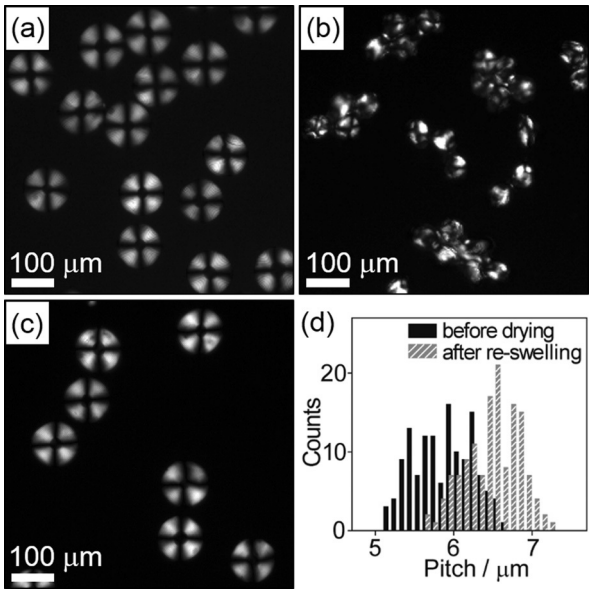

Figure 2. a–c) POM images of large Ch-CNC microgels before drying (a), after drying (b), and following reswelling in water (c). d) Distribution of microgel pitch before drying (black) and after reswelling (gray). a) $D = (105 \pm 3)$ μm, $P = (5.9 \pm 0.4)$ μm; c) $D = (110 \pm 3)$ μm, $P = (6.5 \pm 0.3)$ μm. The error ranges represent the standard deviation.

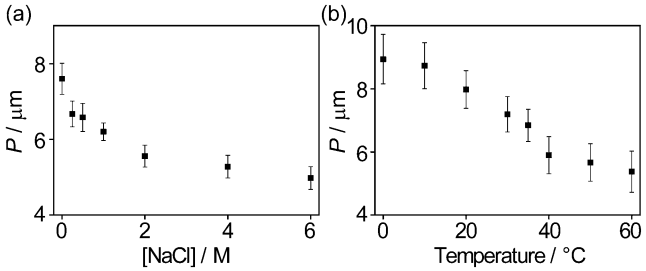

Figure 3. Effect of a) salt concentration and b) temperature on the pitch of large Ch-CNC microgels. The values of *P* were obtained by measuring the pitch of more than 100 microgels. The error bars represent the standard deviation.

P value decreased by 34% (Figure 3a). The shrinkage was caused by the polymer response to the increased ionic strength of the medium: In control experiments, CNC-free PHEA microgels exhibited up to a 62% decrease in the *D* value in 6 M NaCl solution (see Figure S7b). This effect is caused by ion-induced polymer dehydration, which reduces the solubility of the polymer in water (the "salting out" effect).[20]

The less pronounced shrinkage of Ch-CNC versus CNC-free PHEA microgels (see Figure S7a) was attributed to the reinforcement of the polymer network by cross-linking with CNCs. This effect correlated with the reduced contraction of CNC-free poly(HEA) microgels in which the concentration of the cross-linking agent had been increased fourfold (see Figure S7c). Cross-linking of the polymer network with CNCs occurred as a result of hydrogen bonding between the surface hydroxy and sulfate ester groups of the CNCs and hydroxy, carbonyl, and ether groups of the polymer.[21]

We prepared thermoresponsive microgels by emulsifying a mixture of the Ch-CNC phase, *N*-isopropylacrylamide, *N*,*N*′-methylenebisacrylamide, and Irgacure 2595 and subjecting the droplets to UV irradiation. The resulting large microgels had a well-defined Ch morphology, similar to that shown in Figure 1c. Following an increase in temperature of the microgel dispersion from 0 to 60 °C, the microgel pitch decreased by 40% (Figure 3b), with a sharper decrease at about 31 °C, which correlates with the volume phase transition temperature of poly(*N*-isopropylacrylamide) microgels (see Figure S8).[22] Microgel shrinkage at elevated temperature was caused by the increase in the entropic cost of water organization around the polymer, thus reducing its solubility.[20]

The Ch-CNC microgels offered several features indicating their potential as microreactors: 1) the catalytic properties of CNCs in hydrolysis reactions owing to the presence of the nucleophilic hydroxy groups of cellulose;[11a] 2) a negative CNC charge owing to the presence on the CNC surface of sulfate ester groups, which are important for the sequestration of cations in the microgel interior; and 3) a large mesh size[23] and a high surface area of the microgel interior, thus favoring the diffusion of reagents and their transportation into the Ch-CNC microgel.

The catalytic performance of the microgels was examined in the hydrolysis of 4-nitrophenyl acetate, which was added to the microgel dispersion under neutral pH conditions at 15 °C (see the Supporting Information for details). In the course of the reaction, the intensity of the absorption peak at 270 nm of 4-nitrophenyl acetate gradually decreased, and a new peak corresponding to the 4-nitrophenolate ion appeared at 400 nm (Figure 4a).[11a] The reaction occurred significantly faster in the Ch-CNC microgels than in control systems, that is, CNC-free buffer solution (pH 7.4) and a dispersion of CNC-free PHEA microgels (see Figure S9).

In a second series of experiments, the Ch-CNC microgels were used as reactors for the synthesis of metal NPs (Figure 4b), in which the CNCs acted as both a reducing agent and a NP support.[12] The Ch-CNC microgels suspended in a 0.1 M solution of $AgNO_3$ were kept in the dark overnight to introduce Ag^+ ions into the microgel. Following centrifugation of the dispersion and the separation of the supernatant, the microgels were transferred to deionized water and stirred at 80 °C. Within 1 h, the color of the microgel dispersion became yellow, and a plasmon resonance peak at 406 nm evolved in the extinction spectrum (Figure 4b), close to the plasmon resonance of approximately 10 nm Ag NPs.[24] As a control experiment, the procedure described above was repeated for a dispersion of CNC-free PHEA microgels, which remained colorless and showed no distinct features in the spectral range from 300 to 650 nm. Transmission electron microscopy imaging revealed that the resultant Ch-CNC microgels contained (8.0 ± 2.5) nm Ag NPs uniformly distributed in the microgel interior (see Figure S10a–c). Following NP synthesis, the spherical shape and the Ch morphology of the microgels was well-preserved (see Figure S10d).

To explore the catalytic performance of Ag NPs in the microgel interior, hybrid Ch-CNC microgels were added to an aqueous solution of 4-nitrophenol and $NaBH_4$, and the

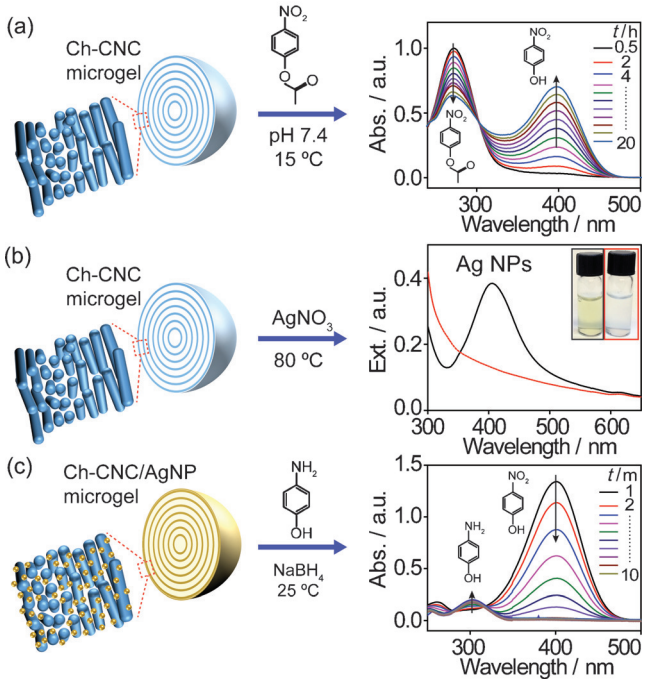

Figure 4. a) Catalytic performance of Ch-CNC microgels in a hydrolysis reaction, with time-dependent absorption spectra of a 0.1 mM aqueous solution of 4-nitrophenyl acetate mixed with a Ch-CNC microgel at 15 °C and pH 7.4. b) Synthesis of Ag NPs in the interior of Ch-CNC microgels, with extinction spectra of a Ch-CNC microgel laden with Ag NPs (black) and a CNC-free PHEA microgel (red). The inset shows aqueous dispersions of Ch-CNC microgels carrying as-synthesized Ag NPs ([Ag NP] = 2.1 nM; left) and CNC-free PHEA microgels (right). c) Catalytic activity of hybrid Ag NP-laden Ch-CNC microgels, with time-dependent absorption spectra of an aqueous solution in which 4-nitrophenol was reduced to 4-aminophenol under the catalysis of Ag NPs ([Ag NP] = 67 pM) in the Ch-CNC microgel interior at 25 °C.

reduction of 4-nitrophenol was monitored at 25 °C by UV/Vis spectroscopy (Figure 4c). The gradual decrease in intensity of the absorption peak of the 4-nitrophenolate ion at 400 nm and the simultaneous appearance of a new peak at 297 nm corresponding to 4-aminophenol[25] were observed for the dispersion of hybrid Ch-CNC microgels. Importantly, owing to the low (< 70 pM) concentration of Ag NPs in this system, their plasmonic band was below the detection limit of the spectrometer, as follows from the spectrum corresponding to the complete reduction of 4-nitrophenol. No significant change in absorbance was observed within the same time interval for the Ch-CNC microgels in the absence of Ag NPs (see Figure S11).

In conclusion, we have developed catalytically active nanofibrillar composite stimulus-responsive microgels. The change in the microgel dimensions and pitch in response to the variation of temperature and ionic strength stemmed from its polymer component. The microgel morphology (predetermined by the CNC organization in the precursor droplets) resulted in the isotropic or anisotropic swelling of microgels with a concentric or planar bipolar CNC organization, respectively. The catalytic performance of the Ch-CNC microgels stemmed from the nucleophilic hydroxy groups on the CNC surface. Furthermore, owing to the negative charge and reducing properties of the CNC component, the Ch-CNC microgels sequestered and reduced Ag^+ ions to plasmonic Ag NPs. The resulting hybrid microgels showed catalytic performance in a reduction reaction. Nanofibrillar CNC microgels offer structural integrity, catalyst retention, and enhanced transportation of molecules to the microgel interior.[26] These features underline the potential of Ch-CNC microgels in catalysis. The combination of these properties paves the way for the design and generation of multifunctional responsive materials with a variety of applications from natural resources.

Acknowledgements

We thank NSERC Canada (Discovery and Strategic Grants) for financial support of this research. Y.L. acknowledges the Banting Postdoctoral Fellowships program, administered by the Government of Canada.

Keywords: cellulose nanocrystals · cholesteric microgels · microreactors · nanoparticles · responsive materials

How to cite: *Angew. Chem. Int. Ed.* **2016**, *55*, 14014–14018
Angew. Chem. **2016**, *128*, 14220–14224

[1] N. M. B. Smeets, T. Hoare, *J. Polym. Sci. Part A* **2013**, *51*, 3027–3043.
[2] a) G. C. Le Goff, R. L. Srinivas, W. A. Hill, P. S. Doyle, *Eur. Polym. J.* **2015**, *72*, 386–412; b) S. Lin, W. Wang, X.-J. Ju, R. Xie, Z. Liu, H.-R. Yu, C. Zhang, L.-Y. Chu, *Proc. Natl. Acad. Sci. USA* **2016**, *113*, 2023–2028.
[3] Y. Gao, W. Xu, M. J. Serpe, *J. Mater. Chem. C* **2014**, *2*, 5878–5884.
[4] a) J. Zhang, S. Xu, E. Kumacheva, *J. Am. Chem. Soc.* **2004**, *126*, 7908–7914; b) J. Zhang, S. Xu, E. Kumacheva, *Adv. Mater.* **2005**, *17*, 2336–2340.
[5] Y. Li, P. Chen, Y. Wang, S. Yan, X. Feng, W. Du, S. A. Koehler, U. Demirci, B.-F. Liu, *Adv. Mater.* **2016**, *28*, 3543–3548.
[6] D. Menne, F. Pitsch, J. E. Wong, A. Pich, M. Wessling, *Angew. Chem. Int. Ed.* **2014**, *53*, 5706–5710; *Angew. Chem.* **2014**, *126*, 5814–5818.
[7] M. Chau, S. E. Sriskandha, H. Thérien-Aubin, E. Kumacheva in *Supramolecular Polymer Networks and Gels*, *Vol. 268* (Ed.: S. Seiffert), Springer International Publishing, Cham, **2015**, pp. 167–208.
[8] a) I. Canton, N. J. Warren, A. Chahal, K. Amps, A. Wood, R. Weightman, E. Wang, H. Moore, S. P. Armes, *ACS Cent. Sci.* **2016**, *2*, 65–74; b) K. A. Simon, N. J. Warren, B. Mosadegh, M. R. Mohammady, G. M. Whitesides, S. P. Armes, *Biomacromolecules* **2015**, *16*, 3952–3958; c) D. Velasco, M. Chau, H. Therien-Aubin, A. Kumachev, E. Tumarkin, Z. Jia, G. C. Walker, M. J. Monteiro, E. Kumacheva, *Soft Matter* **2013**, *9*, 2380–2383.
[9] M. J. Webber, J. Tongers, C. J. Newcomb, K.-T. Marquardt, J. Bauersachs, D. W. Losordo, S. I. Stupp, *Proc. Natl. Acad. Sci. USA* **2011**, *108*, 13438–13443.
[10] a) X. Shen, J. L. Shamshina, P. Berton, G. Gurau, R. D. Rogers, *Green Chem.* **2016**, *18*, 53–75; b) N. E. Mushi, J. Kochumalayil, N. T. Cervin, Q. Zhou, L. A. Berglund, *ChemSusChem* **2016**, *9*, 989–995.
[11] a) T. Serizawa, T. Sawada, H. Okura, M. Wada, *Biomacromolecules* **2013**, *14*, 613–617; b) T. Serizawa, T. Sawada, M. Wada, *Chem. Commun.* **2013**, *49*, 8827–8829.
[12] M. Kaushik, A. Moores, *Green Chem.* **2016**, *18*, 622–637.

[13] J. A. Kelly, A. M. Shukaliak, C. C. Y. Cheung, K. E. Shopsowitz, W. Y. Hamad, M. J. MacLachlan, *Angew. Chem. Int. Ed.* **2013**, *52*, 8912 – 8916; *Angew. Chem.* **2013**, *125*, 9080 – 9084.
[14] Y. Li, J. J. Suen, E. Prince, E. M. Larin, A. Klinkova, H. Therien-Aubin, S. Zhu, B. Yang, A. S. Helmy, O. D. Lavrentovichd, E. Kumacheva, *Nat. Commun.* **2016**, *7*, 12520.
[15] Q. M. Zhang, W. Wang, Y.-Q. Su, E. J. M. Hensen, M. J. Serpe, *Chem. Mater.* **2016**, *28*, 259 – 265.
[16] S. Xu, Z. Nie, M. Seo, P. Lewis, E. Kumacheva, H. A. Stone, P. Garstecki, D. B. Weibel, I. Gitlin, G. M. Whitesides, *Angew. Chem. Int. Ed.* **2005**, *44*, 724 – 728; *Angew. Chem.* **2005**, *117*, 734 – 738.
[17] M. Lee, J. W. Collins, D. M. Aubrecht, R. A. Sperling, L. Solomon, J.-W. Ha, G.-R. Yi, D. A. Weitz, V. N. Manoharan, *Lab Chip* **2014**, *14*, 509 – 513.
[18] D. Seč, T. Porenta, M. Ravnik, S. Žumer, *Soft Matter* **2012**, *8*, 11982 – 11988.
[19] M. Chau, K. J. De France, B. Kopera, V. R. Machado, S. Rosenfeldt, L. Reyes, K. J. W. Chan, S. Förster, E. D. Cranston, T. Hoare, E. Kumacheva, *Chem. Mater.* **2016**, *28*, 3406 – 3415.
[20] Y. Zhang, S. Furyk, D. E. Bergbreiter, P. S. Cremer, *J. Am. Chem. Soc.* **2005**, *127*, 14505 – 14510.
[21] a) M. Tatsumi, Y. Teramoto, Y. Nishio, *Biomacromolecules* **2012**, *13*, 1584 – 1591; b) J. Yang, C.-R. Han, J.-F. Duan, M.-G. Ma, X.-M. Zhang, F. Xu, R.-C. Sun, X.-M. Xie, *J. Mater. Chem.* **2012**, *22*, 22467 – 22480.
[22] B. Zhang, S. Sun, P. Wu, *Soft Matter* **2013**, *9*, 1678 – 1684.
[23] M. Chau, S. E. Sriskandha, D. Pichugin, H. Thérien-Aubin, D. Nykypanchuk, G. Chauve, M. Méthot, J. Bouchard, O. Gang, E. Kumacheva, *Biomacromolecules* **2015**, *16*, 2455 – 2462.
[24] J. Polte, X. Tuaev, M. Wuithschick, A. Fischer, A. F. Thuenemann, K. Rademann, R. Kraehnert, F. Emmerling, *ACS Nano* **2012**, *6*, 5791 – 5802.
[25] J. Tang, Z. Shi, R. M. Berry, K. C. Tam, *Ind. Eng. Chem. Res.* **2015**, *54*, 3299 – 3308.
[26] H. Thérien-Aubin, Y. Wang, K. Nothdurft, E. Prince, S. Cho, E. Kumacheva, *Biomacromolecules* **2016**, DOI: 10.1021/acs.biomac.6b00979.

Received: July 31, 2016
Published online: October 13, 2016

